



The effects of rotation on the surface composition and yields of low mass AGB stars

S. Cristallo, L. Piersanti, and O. Straniero

Istituto Nazionale di Astrofisica – Osservatorio Astronomico di Teramo, Via Maggini snc,
64100 Teramo, Italy, e-mail: cristallo@oa-teramo.inaf.it

Abstract. Over the past 20 years, stellar evolutionary models have been strongly improved in order to reproduce with reasonable accuracy both photometric and spectroscopic observations. Notwithstanding, the majority of these models do not take into account macroscopic phenomena, like rotation and/or magnetic fields. Their explicit treatment could modify stellar physical and chemical properties. One of the most interesting problems related to stellar nucleosynthesis is the behavior of the s-process spectroscopic indexes ([hs/ls] and [Pb/hs]) in Asymptotic Giant Branch (AGB) stars. In this contribution we show that, for a fixed metallicity, rotation can lead to a spread in the [hs/ls] and [Pb/hs] in low-mass AGB stars. In particular, we demonstrate that the Eddington-Sweet and the Goldreich-Schubert-Fricke instabilities may have enough time to smear the ^{13}C -pocket (the major neutron source) and the ^{14}N -pocket (the major neutron poison). In fact, a different overlap between these pockets leads to a different neutrons-to-seeds ratio, with important consequences on the corresponding s-process distributions. Possible consequences on the chemical evolution of Galactic globular clusters are discussed.

Key words. Stars: abundances – Stars: Population II – Stars: nucleosynthesis

1. Introduction

Globular clusters (GCs) have always been considered as the ideal laboratory to test the validity of theoretical evolutionary models. Recently, multiple populations have been detected in many GCs (see Gratton et al. 2012 and references therein), thus implying that they cannot be classified as Simple Stellar Populations. This renewed the interest of the scientific community to these stellar systems. Among the nucleosynthetic features characterizing the different populations of a GC, heavy elements are of particular interest (see, e.g.,

Smith et al. 2000; Yong et al. 2008; Marino et al. 2009). Isotopes heavier than iron ($A \geq 56$) are mainly synthesized by neutron capture processes. The observed distributions show the presence of two main components, correlated to different processes: the s (slow) process and the r (rapid) process. The s-process is mainly active during the Thermally Pulsing AGB (TP-AGB) phase of stars with $1.2 \leq M/M_{\odot} < 4$ Gallino et al. (1998); Straniero et al. (2006). In this phase, freshly synthesized elements are carried out to the surface by means of a recurrent mechanism called Third Dredge Up (TDU). The s-process is characterized by three

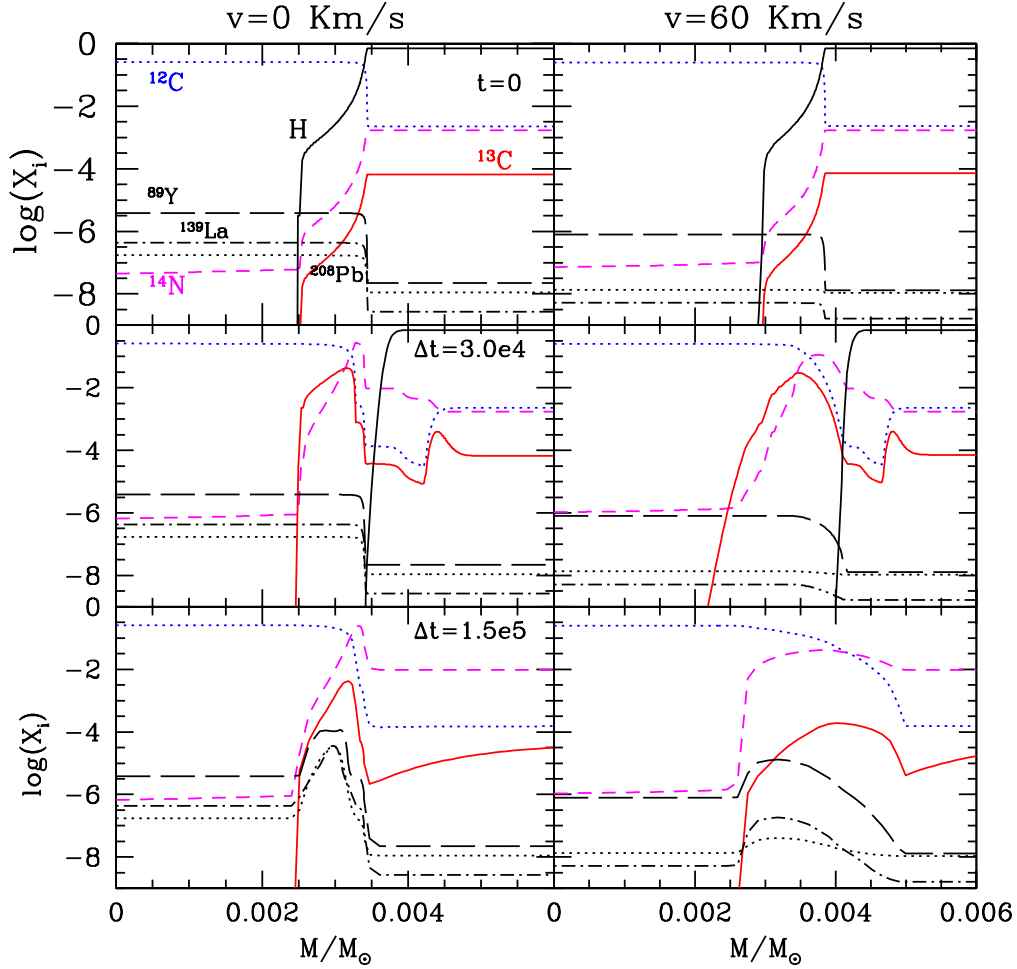


Fig. 1. Temporal evolution of key elements of the $2 M_{\odot}$ model with $[\text{Fe}/\text{H}]=0$ in correspondence of the 3^{rd} ^{13}C pocket forms. A non rotating model and a rotating model are shown.

peaks: the ls^1 , the hs^2 and Pb. Main neutron source of the s-process is the $^{13}\text{C}(\alpha, n)^{16}\text{O}$ reaction, which works in radiative conditions between two Thermal Pulses (TPs). In our models, the introduction of an exponentially decaying profile of convective velocities at the base of the envelope leads to the formation of a self-consistent ^{13}C -pocket. The resulting theoretical s-process distributions are in

¹ $ls=(\text{Sr}, \text{Y}, \text{Zr})$

² $hs=(\text{Ba}, \text{La}, \text{Nd}, \text{Sm})$

agreement with observations, even if a spread of s-process efficiencies at fixed metallicity seems to be requested Cristallo et al. (2009, 2011). The s-process distributions observed in GCs further challenge our knowledge of the s-process nucleosynthesis. One of the most intriguing feature is the particularly low $[\text{Pb}/\text{hs}]^3$ observed in M22 with respect to theoretical models. Among possible solutions to this discrepancy, it has been postulated a contribution

³ $[\text{Pb}/\text{hs}]=[\text{Pb}/\text{Fe}]-[\text{hs}/\text{Fe}]$

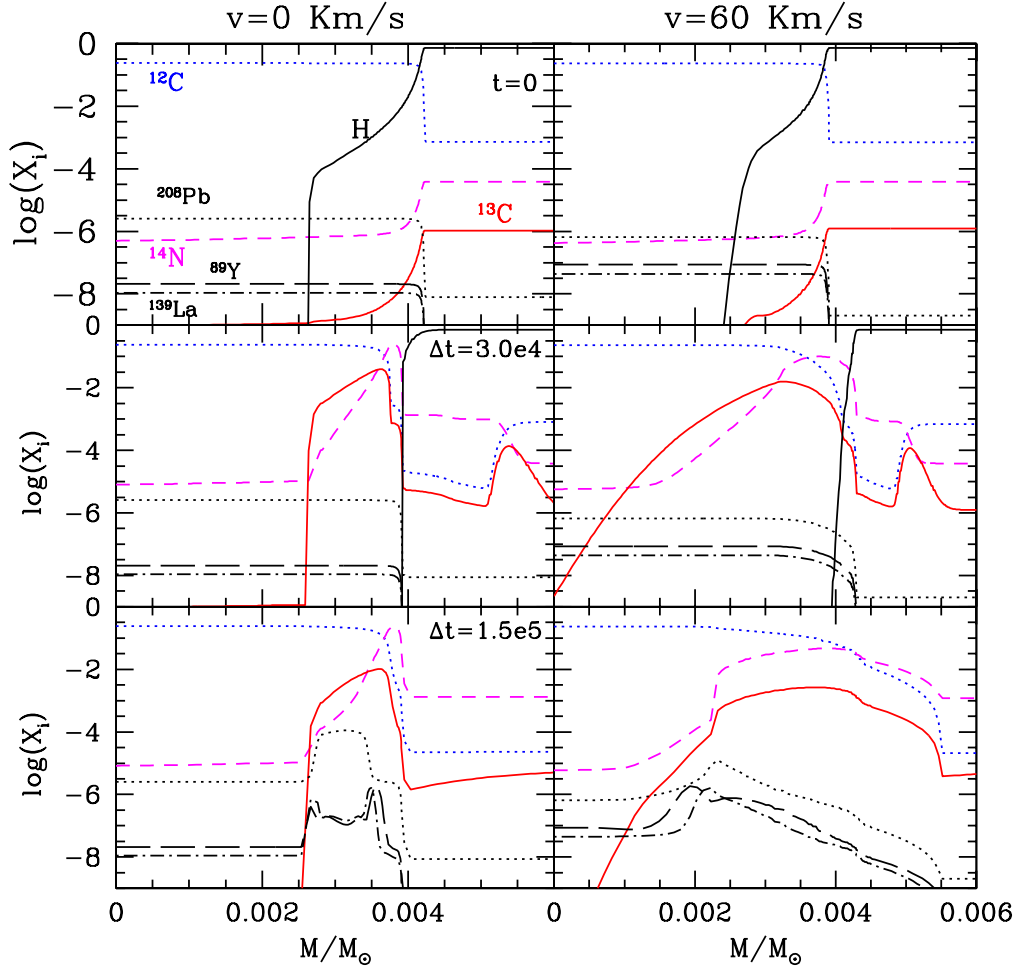


Fig. 2. As in Figure 1, but for a $1.5 M_{\odot}$ model with $[\text{Fe}/\text{H}]=-1.7$ and relative to the 2nd ^{13}C pocket.

from higher (3–4 M_{\odot}) mass AGB models (see Roederer et al. 2011; Straniero et al, *these proceedings*). Alternatively, the contribution from low mass AGB stars could be different. We explore this second hypothesis, by analyzing the effects of rotation on the evolution of these objects.

2. Results

In order to explore the effects of rotation on the physical and chemical AGB evolution we com-

pute models with different masses and metallicities. Models have been computed with the Full-Network Stellar Evolution Code (see Straniero et al. 2006 and references therein). We assign an initial tangential rotational velocity when the star reaches the Zero Age Main Sequence and we describe the evolution of angular momentum through the star via a nonlinear diffusion equation. Details of these models are given in Piersanti et al. 2013. Here we concentrate on two models: a $M=2 M_{\odot}$ model with $[\text{Fe}/\text{H}]=0$ and a $M=1.5 M_{\odot}$ model

with $[\text{Fe}/\text{H}]=-1.7$ ($[\alpha/\text{Fe}]=0.5$), whose metallicities are assumed to be representative of solar neighborhoods and globular clusters, respectively. We found that, during the AGB phase, the introduction of rotation has negligible effects on the physical evolution of the model, but it has deep consequences on the on-going s-process nucleosynthesis. This occurs via the Goldreich-Shubert-Fricke instability (hereafter GSF) and, to a lesser extent, via the Eddington-Sweet circulation (hereafter ES). Both GSF and ES are secular instabilities and, therefore, can work on timescales typical of an AGB interpulse period (some 10^4 yr); their efficiencies are determined by the corresponding velocities (see James & Kahn 1971 for GSF and Kippenhahn 1974 for ES). In Figure 1 we report key elements abundances of the $2 M_{\odot}$ model with $[\text{Fe}/\text{H}]=0$ in the region where the ^{13}C pocket forms. Left panels refer to a non-rotating model, while right panels to a model with initial rotational velocity $v=60 \text{ km s}^{-1}$. Mass coordinates have been scaled to match the same mass interval. Upper panels depict the situation at the maximum penetration of the convective envelope. Intermediate and lower panels show the same stellar layers after 3.0×10^4 yrs (when the ^{13}C and ^{14}N pockets are completely formed) and after 1.5×10^5 yrs (when most of the ^{13}C has already burnt via the $^{13}\text{C}(\alpha, n)^{14}\text{N}$ reaction, thus releasing neutrons), respectively. In the upper part of the ^{13}C pocket, rotation flattens the ^{13}C and ^{14}N profiles via GSF. This instability originates from the inversion in the specific angular momentum profile, as determined by the occurrence of TDU. The inner tail of the ^{13}C -pocket is instead partially mixed by ES. As a consequence, s-process nucleosynthesis occurs on a larger layer with a different efficiency. In particular, the neutron to seed ratio decreases, due to the increased amount of ^{14}N (which is the major neutron poison via its $^{14}\text{N}(n, p)^{14}\text{C}$ resonant reaction). With respect to the non-rotating model, we obtain a reduction of the ls component of about a factor 2 and of the hs component of a factor 3. Consequently, the final $[\text{hs}/\text{ls}]$ index decreases more than 70%. In Figure 2 we report key elements abundances of the $1.5 M_{\odot}$ model with $[\text{Fe}/\text{H}]=-1.7$, in the

region where the $2nd$ ^{13}C pocket forms. As described before, GSF flattens the upper region of the pocket and ES mix the inner tail. In this case, however, the mixing triggered by ES is more efficient. The region where $^{13}\text{C} > ^{14}\text{N}$ increases, thus favoring the production of ls and hs elements. As a net result, in this low metallicity rotating model we obtain a mild decrease of the final $[\text{hs}/\text{ls}]$ index (-70%) and a substantial reduction of the final $[\text{Pb}/\text{hs}]=0.5$ (the non-rotating model is characterized by $[\text{Pb}/\text{hs}]=1.3$).

3. Conclusions

We analyze the effects of rotation on low mass AGB models at different metallicities. At solar metallicity rotation basically determines a decrease of the $[\text{hs}/\text{ls}]$ index, while at low metallicity the major effect is a substantial decrease of the $[\text{Pb}/\text{hs}]$ index. Note that the same effect on the radiative ^{13}C burning is also expected for a slightly larger mass ($M \sim 3 M_{\odot}$) that evolves in a shorter time scale (Straniero et al., *these proceedings*). The latter could be a possible explanation to solve the discrepancy between the $[\text{Pb}/\text{hs}]$ observed in M22 and the higher values predicted by standard non-rotating models.

References

- Cristallo, S., et al. 2009, ApJ, 696, 797
- Cristallo, S., et al. 2011, ApJS, 197, 2
- Gallino, R. et al. 1998, ApJ, 497, 388
- Gratton, R., Carretta E., & Bragaglia, A. 2012, Astron. Astrophys. Rev., 20, 50
- James, R.A., & Kahn, F.D. 1971, A&A, 12, 332
- Kippenhahn, R. 1974, IAUS, 66, 20
- Marino, A.F., et al. 2009, A&A, 505, 1099
- Piersanti, L., Cristallo, S., & Straniero, O., ApJ, submitted
- Roederer, I. U., Marino, A. F., & Sneden, C. 2011, ApJ, 742, 37
- Smith, V.V., et al. 2000, AJ, 119, 1239
- Straniero, O., et al. 2006, Nucl. Phys. A, 777, 311
- Yong, D., et al. 2008, ApJ, 689, 1031